ChemComm
Chemical Communications

Accepted Manuscript

This article can be cited before page numbers have been issued, to do this please use: H. Zhou, S. Duan, J. Huang and F. He, *Chem. Commun.*, 2020, DOI: 10.1039/D0CC01619E.

ROYAL SOCIETY OF CHEMISTRY

rsc.li/chemcomm

ROYAL SOCIETY OF CHEMISTRY
View Article Online
DOI: 10.1039/D0CC01619E

Journal Name

COMMUNICATION

Ultrasensitive electrochemical biosensor for *Pseudomonas aeruginosa* assay based on rolling circle amplification-assisted multipedal DNA walker†

Received 00th January 20xx,
Accepted 00th January 20xx

DOI: 10.1039/x0xx00000x

www.rsc.org/

Huang Zhou, Shaoyun Duan, Ji Huang, and Fengjiao He*

Herein, we developed an ultrasensitive electrochmical biosensor for *Pseudomonas aeruginosa* detection based on rolling circle amplification-assisted multipedal DNA walking strategy. The cascade signal amplification method can improve the sensitivity, showing the promising applications in food security, environment monitoring, and disease diagnostic.

Pseudomonas aeruginosa (*P. aeruginosa*) is a common environmental bacterium that can spread quickly via animal feces, foodstuffs, and water.[1,2] As one of the top three causative agents of opportunistic infections in humans, it has been identified as a vital pathogen by the WHO in 2017, which can result in fearful infections such as otitis, pneumonia, keratitis, septicaemia, and endocarditis.[3] In addition, as one of the most serious society-facing problems, *P. aeruginosa* infection has long been afflicting people around the world. Currently, traditional means for *P. aeruginosa* detection contain plater culture, mass spectrometry, and polymerase chain reaction (PCR). Although these means exhibit excellent sensitivity, large-scale instrument-free and much simpler biosensing platforms are still necessary to develop for *P. aeruginosa* assay.

As we all know, in the field of analytical chemistry, electrochemical method is a classical technology owing to its superiorities of low cost, simplification, high specificity and sensitivity.[4] For instance, the bio-recognition process in the electrochemical biosensing system is simple and efficient, delivering an effective bio-interface without complex operations. Moreover, the cost-effectiveness of the electric (signal) transduction system, such as linear sweep voltammetry (LSV), square wave voltammetry (SWV), and differential pulse voltammetry (DPV), making the whole sensing system applicable in undeveloped area. In view of these advantages, Chen et al. designed an enzyme-free biosensor for electrochemical assay of *P. aeruginosa* using high catalytic Cu-ZrMOF and conductive Super P.[5] On the basis of immunosensing platform, Jayachitra et al. proposed an electrochemical method for *P. aeruginosa* assay via pectin-gold nano-composite.[6] With the adoption of silver nanoparticles-modified glassy carbon electrode, Pourahmad et al. developed an impedimetric aptasensor for *P. aeruginosa* detection.[7] Although these electrochemical biosensors can conquer some drawbacks of the traditional methods to some extent, the low signal amplification efficiency is still hard to meet the needs of practical application. Thus, it is essential to design more sensitive and effective electrochemical biosensor based on signal amplification strategy for *P. aeruginosa* detection.

Over the past decades, to achieve highly sensitive targets detection, a various of very powerful nucleic acid-based signal amplification techniques have been proposed, for example, catalytic hairpin assembly (CHA),[8] rolling circle amplification (RCA),[9] hybridization chain reaction (HCR),[10] strand displacement amplification (SDA),[11] entropy-driven DNA catalysis (EDC),[12] helicase-dependent amplification (HDA),[13] DNA molecular machines,[14] and loop-mediated isothermal amplification (LAMP).[15] Among these above-mentioned nucleic acid-based signal amplification techniques, RCA is often used to build biosensing platforms because of its outstanding signal amplification efficiencies. RCA is a simple and effective isothermal nucleic-acid signal amplification strategy assisted by DNA polymerases, generating some long single-stranded DNAs including abundant complementary duplications of the circular padlock probe.[16,17] Jiang et al. developed a label-free fluorescence biosensing platform for microRNA determination coupling target recycling strategy and RCA.[18] Kong et al. proposed a label-free biosensing platform for telomerase assay through a five-base telomerase product-triggered exponential RCA.[19] Both the RCA-based biosensing platforms can achieve satisfactory signal amplification efficiencies.

As a carrier of genetic information, it is well known that DNA is considered to be the most promising type of material for molecular machine construction, not only due to the good

State Key Laboratory of Chemo/Biosensing and Chemometrics, College of Chemistry and Chemical Engineering, Hunan University, Changsha, 410082, P. R. China. E-mail: fengjiao87799232@hotmail.com

†Electronic Supplementary Information (ESI) available. See DOI: 10.1039/x0xx00000x

biocompatibility of endogenous substances, but also due to the certain advantages compared to other materials, such as precise base pairing principles, sequence programmability, structural diversity and controllability, mature synthesis techniques and easy to modify.[20] Using DNA as a construction element, researchers designed and prepared a variety of DNA molecular nanomachines, containing DNA tweezers,[21] DNA motors,[22] DNA gears,[23] DNA robots,[24] DNA scissor,[25] and DNA walkers.[26] Among these DNA machines, DNA walker is identified as an attractive nucleic acid-based amplification method, which can move automatically along assembled nucleic acid-tracks powered by nicking endonuclease,[27,28] DNAzymes[26,29] or strand displacement,[30] resulting in excellent signal amplification. Ju et al. developed a binding-induced electrochemical biosensor for thrombin detection based on unipedal DNA walker.[31] Miao et al. developed an electrochemical biosensing system for target DNA detection based on bipedal DNA walker.[32] In order to further improve the sensitivity of biosensing system, He et al. developed a four-leg DNA walker coupled with CHA for streptavidin detection.[33] Although these DNA walker-based biosensors provide new methods for target determination, the adoption of a limited number of legs restricts the further improvement of sensitivity. Therefore, to obtain better analytical performance, it is indeed necessary to propose a biosensor based on multipedal DNA walking strategy for sensitive target assay. Recently, Tang et al. proposed a gold nanoparticles-based multipedal DNA walker for electrochemical ratiometric biosensor for circulating tumor cell assay, and the detection limit is down to 1 cell/mL.[34] In order to further improve the sensitivity, cascade signal amplification should be introduced in the biosensors by combining RCA and multipedal DNA walking strategy. The combination has two main advantages: One is that the nucleic acid strands can be extensively expanded after RCA reaction to provide abundant binding sites for DNA legs. On the other hand, plentiful DNA legs bind to the RCA products to form multipedal DNA walker, finally obtaining a high turnover for signal amplification. Therefore, an electrochemical biosensing platform based on the above cascade signal amplification strategy is greatly deserved to be studied for bacteria detection.

As we all know, the 16S rRNA is composed of the conserved and variable region, and the conserved region is very stable and suitable for universal bacteria assay. In the present work, inspired by the advantages of RCA and DNA walker strategies, we were the first to develop an electrochemical biosensing platform based on RCA reaction and multipedal DNA walking strategy for cascade signal amplification assay of the conserved region of 16S rRNA gene from *P. aeruginosa* (Scheme 1). First, the methylene blue (MB)/SH-modified signal probes (SP) and SH-modified capture probes (CP) are fabricated on the gold (Au) electrode surface via Au-S bond, which is then passivated by 6-mercaptohexanol (MCH) to avoid non-specific adsorption. In the presence of 16S rRNA, the 16S rRNA will hybridize with CP. Then, the auxiliary probe (AP) was added to the Au electrode surface. After the hybridization of 16S rRNA with AP and the addition of the circular padlock probe (CPP), phi29 polymerase, and dNTPs, the RCA reaction was triggered to generate many repeated sequences partially complementary with walker probe (WP), leading to the formation of multipedal DNA walker. Subsequently, with the addition of Pb^{2+}, the multipedal walking procedure is conducted and the SP is cleaved by the Pb^{2+}-dependent DNAzyme, finally resulting in the reduce in the peak current of MB. On the basis of the cascade signal amplification by coupling RCA reaction and multipedal DNA walker strategies, the proposed electrochemical biosensor displays superior analytical performance for *P. aeruginosa* with the detection limit of 10 CFU/mL. In addition, when the developed biosensor was employed to identify *P. aeruginosa* in 45 clinical sputum samples, there was no obvious difference compared with those tested by the culture method. Therefore, the proposed electrochemical biosensing platform provides a promising tool for rapid determination of *P. aeruginosa* and has great potential application in food safety, environmental monitoring, and disease diagnosis.

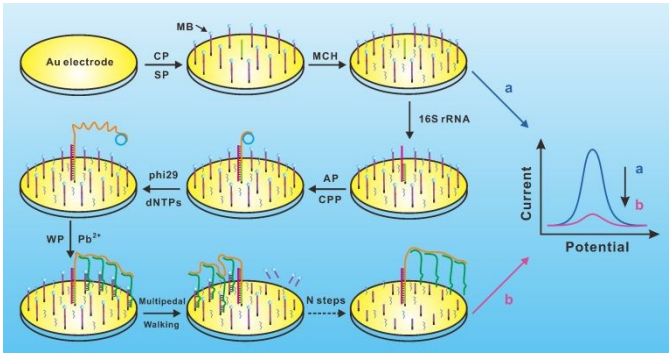

Scheme 1 Schematic illustration of the electrochemical biosensor based on RCA and multipedal DNA walking strategy.

First, electrochemical impedance spectroscopy (EIS) was applied to characterize the fabrication process of the electrochemical biosensor. In the classical EIS, the semicircle diameter at higher frequency is relevant to the electron transfer process and its enhancement demonstrates the increase of the interfacial charge transfer resistance (R_{ct}).[35] As exhibited in Fig. 1A, compared to bare Au electrode (curve a), the R_{ct} value increased after the modification of SP and CP due to the strong repulsion effect between the negatively charged SP-CP and $[Fe(CN)_6]^{3-/4-}$ (curve b). Next, after the above electrode was incubated in MCH, there was an evident augment of the R_{ct} value (curve c). When the 16S rRNA, AP and CPP sequentially were modified on the electrode surface, a gradual increase of Rct values were observed (curves d and e). After RCA reaction, the R_{ct} value enhanced remarkably due to the extension of AP strands (curve f). Furthermore, the R_{ct} value increased owing to the hybridization of WP with the extended AP strands (curve g). Whereas, it decreased after the multipedal walking process and cleavage reaction (curve h). Simultaneously, the cyclic voltammetry (CV, scan rate: 0.1 V/s) results also confirmed the stepwise modification of the biosensor. As displayed in Fig. 1B, the bare Au electrode showed a pair of well-defined peaks because of its excellent electric conduction (curve a). After the fabrication of SP and CP, an obvious reduce in current response and an increase of peak separation can be observed because of the strong repulsion effect between the negatively charged SP-CP and $[Fe(CN)_6]^{3-/4-}$ (curve b). After the sequential modification of MCH, 16S rRNA, AP and CPP, the current responses decreased gradually (curves c to e). After RCA reaction, there

was a remarkable decrease of the current response, which may be due to the extension of AP strands (curve f). The current response further decreased owing to the hybridization of WP with the extend AP strands (curve g). However, it increased after the multipedal walking process and cleavage reaction (curve h). These CV results in Fig. 1B were in agreement with that displayed in the EIS analysis, indicating the successful fabrication of the designed electrochemical biosensing system.

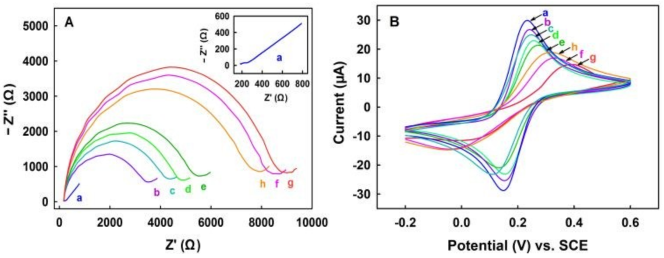

Fig. 1 Investigation of the modification steps using EIS performed in 0.1 M KCl aqueous solution containing 5 mM (1:1) $[Fe(CN)_6]^{3-/4-}$ in the frequency range from 0.1 Hz to 100 kHz with 5 mV as the amplitude at a potential of 0.22 V (A) and CV (B) curves of (a) bare Au electrode, (b) SP-CP/Au electrode, (c) MCH/SP-CP/Au electrode, (d) 16S rRNA/MCH/SP-CP/Au electrode, (e) AP/16S rRNA/MCH/SP-CP/Au electrode, (f) AP/16S rRNA/MCH/SP-CP/Au electrode after RCA reaction, (g) Electrode of (f) after the addition of WP, (h) Electrode of (g) after multipedal DNA walking process.

Next, in order to verify the feasibility, the DPV technology was employed. As shown in Fig. S1, compared to the current peak of the MCH/SP-CP/Au electrode (curve a), in the absence of 16S rRNA, no obvious change in peak current was observed after the MCH/SP-CP/Au electrode was incubated in the RCA system and Pb^{2+}-dependent DNAzyme cleavage system (curve b). However, in the presence of 10 pM 16S rRNA, the peak current reduced observably (curve c), indicating a satisfactory feasibility of the developed electrochemical biosensing system.

Because the analysis performance of the developed biosensing platform is vastly influenced by analysis conditions, some crucial experimental parameters should be investigated. First, the ratio of SP/CP was investigation from 1 to 40 in the presence of 0.1 nM 16S rRNA. As exhibited in Fig. S2A, with the increase of CP concentration, the peak current of MB decreased because of the competitive effect between CP and SP during the self-assembly of DNA monolayer. Nevertheless, low concentration of CP had a vital influence on the sensitivity of target recognition. Hence, the SP concentration with 20-fold higher than CP concentration was chosen as self-assembled multipedal DNA walker track. The RCA reaction time is another crucial parameter for the extension of RCA products. As exhibited in Fig. S2B, the peak current of MB decreased with the enhancement of reaction time and achieved a platform at the time of 1.5 h in the presence of 0.5 nM 16S rRNA, therefore, 1.5 h was used as the optimized reaction time. Additionally, some parameters are also very vital to the multipedal DNA walking process that may affect the hybridization kinetics and the DNAzyme cleavage efficiency directly, such as complementary base number, Pb^{2+} concentration, reaction temperature, and reaction time. In the study, the 3′-end of the DNAzyme tail is immobilized through 5 bases, and the length of 5′-end are in the range from 5 to 9 bases. Ideally, the nonspecific cleavage can be reduced to some extent by a shorter DNAzyme tail; whereas, it is hard to reach specific signal intensity for a too short DNAzyme tail. While the DNA duplex formed by an overlength of DNAzyme tail can generate a strong false positive signal. As displayed in Fig. S2C, the peak current of MB decreased gradually in the absence of 16S rRNA due to the non-specific cleavage with the enhancement of complementary base number on the 5′-end of the DNAzyme tail, and the signal-to-noise ratio reached a maximum value when the base number was six. Therefore, the DNAzyme tail with 6 bases was used in the work. In addition, the Pb^{2+} concentration, cleavage temperature, and cleavage time were also evaluated, respectively (Fig. S2D, E, and F).

Under optimized experimental parameters, we investigated the sensitivity of the designed electrochemical method with varied 16S rRNA concentrations ranging from 10 fM to 10 nM. As exhibited in Fig. 2A, the peak current of MB reduced with the enhancement of 16S rRNA concentrations. Moreover, the peak current was linear with the logarithmic concentration of 16S rRNA ranging from 10 fM to 1 nM (Fig. 2B). The regression equation was $I = -0.1054 \lg C_{16S\ rRNA} + 0.3548$ ($R^2 = 0.9982$) with the detection limit of 10 fM, verifying the excellent analytical performance for 16S rRNA assay.

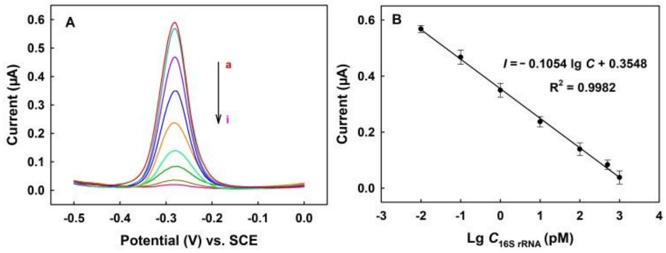

Fig. 2 (A) DPV responses of the electrochemical biosensor with different concentrations of 16S rRNA. (a–i) 0 fM, 10 fM, 100 fM, 1 pM, 10 pM, 100 pM, 1 nM, 5 nM, and 10 nM. (B) Corresponding calibration plot of DPV peak current vs logarithm of 16S rRNA concentration. Error bars represent the standard deviation of three individual assays.

Subsequently, the stability of the proposed electrochemical biosensing platform was investigated by storing the biosensing electrodes at 4 °C for two weeks, three parallel measurements demonstrated that they could keep about 97.6% of their original peak currents for 16S rRNA assay. Subsequently, the reproducibility was evaluated by measuring five biosensing electrodes in the presence of 10 pM 16S rRNA, and the relative standard deviation was only 3.8%, verifying a satisfactory reproducibility. Additionally, the specificity of the proposed biosensing platform was also investigated by DPV method using four kinds of RNA sequences, including 16S rRNA (0.5 nM), single-base mismatched RNA (1MM, 5 nM), three-base mismatched RNA (3MM, 5 nM), and non-complementary RNA (NC, 5 nM). As exhibited in Fig. S3, the peak current of MB for 16S rRNA was only about 22.4% and 17.4% of that for 1MM and 3MM, respectively. The NC sequence exhibited almost the same peak current as the blank control. These results demonstrated that the designed biosensing platform has outstanding specificity for 16S rRNA assay. Furthermore, the recovery test was also performed, as shown in Table S1, the recovery varied from 98.6% to 103.0%, demonstrating that the proposed electrochemical biosensing system has the potential to be used in real biological samples.

The electrochemical responses of different concentrations of *P. aeruginosa* are shown in Fig. 3A. With the increase of *P. aeruginosa* concentrations, the peak current of MB decreased ranging from 10 to 1×10^9 CFU/mL. Moreover, the peak current was linear with the logarithmic concentration of *P. aeruginosa* ranging from 10 to 1×10^8 CFU/mL (Fig. 3B). The regression equation was $I = -0.0761 \lg C_{pa} + 0.6243$ ($R^2 = 0.9866$) with a

View Article Online
DOI: 10.1039/D0CC01619E

detection limit of 10 CFU/mL, indicating the outstanding analysis capability for *P. aeruginosa* detection than other reported analytical methods (Table S2).

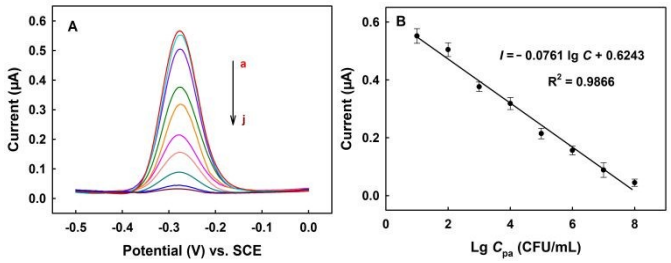

Fig. 3 (A) DPV responses of the electrochemical biosensor to 16S rRNA from different concentrations of *P. aeruginosa*. (a–j) 0, 10, 1×10^2, 1×10^3, 1×10^4, 1×10^5, 1×10^6, 1×10^7, 1×10^8, and 1×10^9 CFU/mL. (B) Corresponding calibration plot of DPV peak current vs logarithm of *P. aeruginosa* concentration. Error bars represent the standard deviation of three individual assays.

In order to evaluate the selectivity toward 16S rRNA of the proposed electrochemical biosensing platform, a variety of potential interfering bacteria including *S. aureus*, *E. sakazakii*, *S. typhimurium*, *L. monocytogenes*, and *V. parahaemolyticus* were measured at the concentration of 1×10^8 CFU/mL. As shown in Fig. S4, almost no change of peak current can be observed in the presence of interfering bacteria and it was only in the presence of *P. aeruginosa* that the peak current decreased significantly, indicating a satisfactory selectivity of the proposed electrochemical biosensing platform for *P. aeruginosa*. Finally, the practicability of the designed electrochemical biosensor was evaluated by employing 45 simulated sputum samples containing 14 positive samples and 31 negative samples for *P. aeruginosa* identification through conventional bacteria culture method (Table S3).

In the work, a novel and sensitive electrochemical biosensing platform was successfully developed for cascade signal amplification assay of *P. aeruginosa* by coupling RCA reaction and multipedal DNA walking strategy. The adoption of abundant legs of multipedal DNA walking strategy further improved the sensitivity with the detection limit of 10 CFU/mL. The proposed electrochemical biosensing platform provides a promising tool for sensitive determination of *P. aeruginosa* and has great potential application in food security, environment monitoring, and disease diagnostic.

This work was supported by the National Natural Science Foundation of China (Grant No. 21275042).

Conflicts of interest

There are no conflicts to declare.

Notes and references

1 R. Frei, A. S. Breitbach and H. E. Blackwell, *Angew. Chem. Int. Ed.*, 2012, **51**, 5226–5229.
2 B. K. Gorityala, G. Guchhait, D. M. Fernando, S. Deo, S. A. McKenna, G. G. Zhanel, A. Kumar and K. Schweizer, *Angew. Chem. In. Ed.*, 2016, **55**, 555–559.
3 M. W. Silby, C. Winstanley, S. A. C. Godfrey, S. B. Levy and R. Jackson, *FEMS Microbiol. Rev.*, 2011, **35**, 652–680.
4 E. H. Xiong, Z. Z. Li, X. H. Zhang, J. W. Zhou, X. X. Yan, Y. Q. Liu and J. H. Chen, *Anal. Chem.*, 2017, **89**, 8830–8835.
5 X. Zhang, G. M. Xie, D. Gou, P. Luo, Y. Yao and H. Chen, *Biosens. Bioelectron.*, 2019, **142**, 111486.
6 N. Krithiga, K. B. Viswanath, V. S. Vasantha and A. Jayachitra, *Biosens. Bioelectron.*, 2016, **79**, 121–129.
7 M. Roushani, M. Sarabaegi and F. Pourahmad, *Microchim. Acta*, 2019, **186**, 725.
8 Z. Wu, G. Q. Liu, X. L. Yang and J. H. Jiang, *J. Am. Chem. Soc.*, 2015, **137**, 6829–6836.
9 S. N. Wang, Y. H. Ji, H. M. Fu, H. X. Ju and J. P. Lei, *Analyst*, 2019, **144**, 691–697.
10 X. M. Shi, G. C. Fan, X. Y. Tang, Q. M. Shen and J. J. Zhu, *Biosens. Bioelectron.*, 2018, **109**, 190–196.
11 W. S. Saisuk, C. Srisawat, S. Yoksan and T. Dharakul, *Anal. Chem.*, 2019, **91**, 3286–3293.
12 F. Ma, S. H. Wei and C. Y. Zhang, *Anal. Chem.*, 2019, **91**, 7505–7509.
13 F. Ma, M. Liu, B. Tang and C. Y. Zhang, *Anal. Chem.*, 2017, **89**, 6182–6187.
14 P. Q. Ma, C. P. Liang, H. H. Zhang, B. C. Yin and B. C. Ye, *Chem. Sci.*, 2018, **9**, 3299–3304.
15 M. Varona and J. L. Anderson, *Anal. Chem.*, 2019, **91**, 6991–6995.
16 X. J. Kong, S. Wu, Y. Cen, R. Q. Yu and X. Chu, *Biosens. Bioelectron.*, 2016, **79**, 679–684.
17 T. Ye, J. Y. Chen, Y. F. Liu, G. H. Zhou and Z. He, *ACS Appl. Mater. Interfaces*, 2014, **6**, 16091–16096.
18 T. T. Fan, Y. Mao, F. Liu, W. Zhang, J. S. Lin, J. X. Yin, Y. Tan, X. T. Huang and Y. Y. Jiang, *Talanta*, 2019, **200**, 480–486.
19 X. Y. Li, Y. X. Cui, Y. C. Du, A. N. Tang and D. M. Kong, *ACS Sens.*, 2019, **4**, 1090–1096.
20 J. S. Shin and N. A. Pierce, *J. Am. Chem. Soc.*, 2004, **126**, 10834–10835.
21 M. H. Liu, J. L. Fu, C. Hejesen, Y. H. Yang, N. W. Woodbury, K. Gothelf, Y. Liu and H. Yan, *Nat. Commun.*, 2013, **4**, 2127.
22 T. G. Cha, J. Pan, H. R. Chen, J. Salgado, X. Li, C. D. Mao and J. H. Choi, *Nat. Nanotechnol.*, 2014, **9**, 39–43.
23 Y. Tian and C. D. Mao, *J. Am. Chem. Soc.*, 2004, **126**, 11410–11411.
24 Y. Y. Chang, Z. Y. Wu, Q. X. Sun, Y. Zhuo, Y. Q. Chai and R. Yuan, *Anal. Chem.*, 2019, **91**, 8123–8128.
25 L. C. Peng, Y. L. Yuan, X. M. Fu, A. Fu, P. Zhang, Y. Q. Chai, X. X. Gan and R. Yuan, *Anal. Chem.*, 2019, **91**, 3239–3245.
26 L. Zhao, R. J. Sun, P. He and X. R. Zhang, *Anal. Chem.*, 2019, **91**, 14773–14779.
27 D. Long, M. J. Li, H. H. Wang, H. J. Wang, Y. Q. Chai and R. Yuan, *Biosens. Bioelectron.*, 2019, **142**, 111579.
28 Y. Y. Li, G. A. Wang, S. D. Mason, X. L. Yang, Z. C. Yu, Y. N. Tang and F. Li, *Chem. Sci.*, 2018, **9**, 6434–6439.
29 C. Liu, Y. L. Hu, Q. S. Pan, J. T. Yi, J. Zhang, M. M. He, M. Y. He, T. T. Chen and X. Chu, *Biosens. Bioelectron.*, 2019, **136**, 31–37.
30 C. Jung, P. B. Allen and A. D. Ellington, *ACS Nano*, 2017, **11**, 8047–8054.
31 Y. H. Ji, L. Zhang, L. Y. Zhu, J. P. Lei, J. Wu and H. X. Ju, *Biosens. Bioelectron.*, 2017, **96**, 201–205.
32 H. Chai and P. Miao, *Anal. Chem.*, 2019, **91**, 4953–4957.
33 N. N. Li, M. Y. Du, Y. C. Liu, X. H. Ji and Z. K. He, *ACS Sens.*, 2018, **3**, 1283–1290.
34 P. Miao and Y. G. Tang, *Anal. Chem.*, 2019, **91**, 15187–15192.
35 Y. Cao, S. Zhu, J. C. Yu, X. J. Zhu, Y. M. Yin and G. X. Li, *Anal. Chem.*, 2012, **84**, 4314–4320.

View Article Online
DOI: 10.1039/D0CC01619E

Graphical Abstract

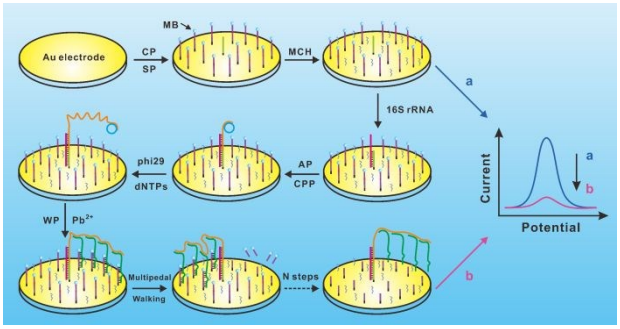

Ultrasensitive electrochemical biosensor for *Pseudomonas aeruginosa* assay based on rolling circle amplification-assisted multipedal DNA walker

Highlights

- An ultrasensitive electrochemical biosensor was developed based on RCA and multipedal DNA walking strategy for cascade signal amplification assay of 16S rRNA gene from *Pseudomonas aeruginosa*.
- The developed electrochemical biosensor provides a novel, sensitive, and accurate platform for *Pseudomonas aeruginosa* detection.
- The electrochemical biosensor shows excellent analytical performance, and has great potential application in food safety, environmental monitoring, and disease diagnosis.